Dislocation climb strengthening in systems with immobile obstacles: Three-dimensional level-set simulation study

Zi Chen,[1,2] Kevin T. Chu,[2,3,4] David J. Srolovitz,[4] Jeffrey M. Rickman,[5,6] and Mikko P. Haataja[1,2,7]
[1]*Department of Mechanical and Aerospace Engineering, Princeton University, Princeton, New Jersey 08540, USA*
[2]*Princeton Institute for the Science and Technology of Materials (PRISM), Princeton University, Princeton, New Jersey 08540, USA*
[3]*Vitamin D, Inc., Menlo Park, California 94025, USA*
[4]*Institute of High Performance Computing, Singapore, Singapore*
[5]*Department of Materials Science and Engineering, Lehigh University, Bethlehem, Pennsylvania 18015, USA*
[6]*Department of Physics, Lehigh University, Bethlehem, Pennsylvania 18015, USA*
[7]*Program in Applied and Computational Mathematics (PACM), Princeton University, Princeton, New Jersey 08540, USA*
(Received 20 February 2009; revised manuscript received 30 December 2009; published 3 February 2010)

We employ a parallel, three-dimensional level-set code to simulate the dynamics of isolated dislocation lines and loops in an obstacle-rich environment. This system serves as a convenient prototype of those in which extended, one-dimensional objects interact with obstacles and the out-of-plane motion of these objects is key to understanding their pinning-depinning behavior. In contrast to earlier models of dislocation motion, we incorporate long-ranged interactions among dislocation segments and obstacles to study the effect of climb on dislocation dynamics in the presence of misfitting penetrable obstacles/solutes, as embodied in an effective climb mobility. Our main observations are as follows. First, increasing climb mobility leads to more effective pinning by the obstacles, implying increased strengthening. Second, decreasing the range of interactions significantly reduces the effect of climb. The dependence of the critical stress on obstacle concentration and misfit strength is also explored and compared with existing models. In particular, our results are shown to be in reasonable agreement with the Friedel-Suzuki theory. Finally, the limitations inherent in the simplified model employed here, including the neglect of some lattice effects and the use of a coarse-grained climb mobility, are discussed.

DOI: 10.1103/PhysRevB.81.054104 PACS number(s): 61.72.Lk, 61.72.Yx, 62.20.F−

I. INTRODUCTION

The study of dynamical critical phenomena associated with the pinning-depinning transition in random media has become a subject of considerable interest in recent decades.[1] This interest is due to the importance of pinning in a variety of important physical systems such as vortex flux lines in type-II superconductors,[2] domain walls in magnetic or ferroelectric materials,[3,4] charge-density waves,[5] contact lines,[6] and propagating cracks in solids.[7] In particular, the toughening of epoxies often involves the pinning of crack fronts[8] and the magnetic properties of samarium-based magnets arise from the pinning of domain walls by precipitates produced by isothermal aging.[9]

In describing the interaction of an object with pinning obstacles, it is of interest to characterize the influence of the obstacles on the object's trajectory. In some cases, it is found that transverse motion of a one-dimensional object is an essential feature of its dynamics. For example, in the aforementioned type-II superconductors, the measured Hall resistance embodies the transverse motion of vortices as they move outside of the channels in which they flow.[10] Moreover, in anisotropic type-II superconductors, it has been shown that the critical force for the motion of vortices may be smaller than pinning forces as vortex motion can be at an angle with respect to the force.[11] In the case of propagating cracks, a pinned crack can bypass obstacles by an in-plane bowing process or by an out-of-plane deflection of the crack tip due to local stresses at the obstacle.[12]

Pinning phenomena also play an important role in physical metallurgy, especially in heavily worked metals[13,14] containing dislocations, and here again (line) objects can bypass pinning obstacles via transverse motion. In this case, dislocation climb is a nonconservative dynamics facilitated by the long-ranged diffusion of point defects toward and away from a dislocation line,[15] and may provide pathways around obstacles that hinder the motion of driven lines. A knowledge of the mechanisms involved in dislocation pinning and bypass is of both scientific and technological importance as many advanced metallic systems have been tailored to enhance their strength and/or other mechanical properties via the introduction of solutes or other phases that act as pinning obstacles to dislocation motion. For example, in systems that are solution and/or precipitation hardened, such as TiAl and Al-Mg-Cu alloys and reinforced $MoSi_2$,[16–20] interactions between dislocations and other defects lead to a complex plastic response that is difficult to capture by empirical constitutive relations. This complexity can be traced to the multitude of possible dislocation conformational changes associated with the driven motion of line defects in a sea of obstacles. Moreover, in some stress regimes, the interaction of mobile and immobile solutes with moving dislocations can lead to a rich set of phenomena, such as the dynamical pinning/unpinning associated with the Portevin-LeChatelier effect that is thought to be responsible for serrated stress-strain curves in many nonferrous alloys.[21] Thus, a more complete picture of crystal plasticity in hardened metals requires a better understanding of operative dislocation/obstacle interaction mechanisms and, in particular, an appreciation of the role of dislocation climb in obstacle bypass processes.

As a specific illustration of the impact of transverse motion on the depinning of defects, we focus here on the me-

soscale simulation of particle-strengthened materials in which dislocations and pinning particles are the entities of interest, and the energetics follows from continuum elasticity. The advent of dislocation dynamics (DD) simulations[22–27] in both two and three spatial dimensions has led to insights into the cooperative motion of multiple dislocations and the formation of dislocation substructures. In addition, recent Monte Carlo studies of overdamped dislocation motion in the presence of both mobile and immobile obstacles in two dimensions[28,29] have successfully demonstrated many of the essential features of strain aging and dislocation pinning. While these phenomena can be described approximately using such simplified models based on rigid dislocation lines, a more general treatment necessitates an extension of dislocation dynamics simulation to include degrees of freedom associated with dislocation loop conformations as well as dislocation-solute interactions. The level-set method for dislocation dynamics[30–32] offers a promising avenue for modeling dislocation interaction with obstacles including the topological changes associated with dislocation climb, cross slip and loop formation. This approach to DD, outlined in some detail below, will be employed in this study to highlight especially the role of climb mobility in dislocation/obstacle interactions.

Previous studies have assessed the impact of a random distribution of obstacles on dislocation glide within a simple line tension description of dislocations (where a dislocation is modeled as an elastic string).[33,34] In their early work, Foreman and Makin[35] examined the glide of a string in an environment of point particles to obtain the dependence of the critical resolved shear stress on the properties of the particle distribution in two dimensions. More recently, Nogaret and Rodney[36] reconsidered this model to deduce corrections to the critical stress associated with finite-sized arrays of obstacles. While the motion of an elastic string through a field of obstacles captures the essence of dislocation pinning and depinning mechanisms, the aforementioned level-set method permits a more realistic description of these mechanisms as it naturally incorporates both dislocation glide and climb, and properly reflects the long-ranged elastic interactions inherent in dislocation-particle dynamics. In particular, as noted above, dislocation climb is important here as it facilitates obstacle bypass mechanisms, and elastic interactions are especially relevant as they dictate favorable dislocation/obstacle configurations.

Before examining the impact of climb in this context, we first review the salient features of the generic, statistical problem of solid-solution hardening via dislocation pinning. To this end, two trends have been observed in the evolution of theories of solid-solution hardening.[37,38] In the first, typified by the classic paper of Mott and Nabarro,[39] noninteracting dislocations move under an applied shear stress in a piecewise fashion through random dispersions of localized, pointlike, attractive and repulsive barriers. This model is collective in the sense that the solute concentration, c, is high enough that each dislocation segment may be assumed to be interacting with several solute atoms while it advances. By contrast, in the second type of breakaway model, such as that of Friedel,[21] a low solute concentration facilitates breakaway from individual pinning centers. In their pioneering work, Mott and Nabarro[39] obtained the critical shear stress (σ_c) dependence on concentration as $\sigma_c \sim c^{5/3}(\log c)^2$, assuming that the solute atoms are uniformly distributed and that a dislocation interacts with the internal stress field of dispersed, weak obstacles.

Labusch[40,41] introduced the concept of a "cluster of obstacles" and proposed a statistical theory of solid-solution hardening that gives the often observed $c_0^{2/3}$ relation[42] for the concentration dependence of the flow stress: $\sigma_c \sim (f_m^4 c_0^2 w/T)^{1/3}$, where c_0 is the areal concentration, T is the line tension, f_m is the maximum dislocation-obstacle interaction force, and w is the range of interaction. Nabarro reexamined the basic features of solid-solution hardening and suggested that a sufficiently dilute solid solution permits arcs in dislocation lines to break away from pinning points (i.e., in the "Friedel limit"[21]), leading to $\sigma_c \sim (f_m^3 c_0/T)^{1/2}$.[43] At high concentrations, the solute atoms will be closely spaced along the dislocation line, implying that the breakaway-and-repinning process involves a dislocation segment interacting with many obstacles; for this scenario he derived the scaling law $\sigma_c \sim (f_m^4 c_0^2 w/T)^{1/3}$. We note that this dependence of σ_c on c_0 and f_m is exactly the same as in Labusch's theory. Yet another theory proposed by Friedel[21] and Suzuki[44] allows the dislocation line to attain much larger local curvatures than in previous models. This theory predicts that $\sigma_c \sim f_m c_0$, independent of the line tension in contrast to the other theories. Furthermore, the Friedel-Suzuki theory was shown to be in good agreement with recent atomistic simulation results.[45] These predicted scaling relations provide the basis for a quantitative analysis of our simulation results.

The aim of this paper is, then, to investigate the overdamped motion of an initially straight edge dislocation through an array of misfitting obstacles as a function of obstacle concentration and spatial distribution, misfit strain, and external stress to highlight the role of climb in dislocation/obstacle interactions. This system serves as a convenient prototype of those in which extended, mobile objects interact with obstacles and the out-of-plane motion of these objects is key to understanding their pinning-depinning behavior. More specifically, from these studies, we extract the effective glide mobility of the dislocation and assess the effect of dislocation climb mobility on critical applied shear stress. As will be seen below, we find, counterintuitively, that a greater climb mobility decreases the effective glide mobility. This interesting behavior is rationalized in terms of long-ranged dislocation-obstacle interactions. It is worth noting that previous models assume that the dislocation-obstacle interactions are short ranged, while in the current work, the full long-ranged dislocation-obstacle interactions are naturally incorporated. Therefore, we also examine the dependence of the strengthening effect on the range of the interaction.

The remainder of this paper is organized as follows. In the next section, we use a heuristic model to study dislocation motion (both glide and climb) through a regular array of misfitting circular inclusions; a quasi-two-dimensional (2D) dynamics problem. While this approach provides some guidance in understanding the effects of climb, its two-dimensional nature limits its applicability to the three-dimensional (3D) problem of interest. Subsequently, we present a three-dimensional dislocation dynamics model

based on the level-set method that incorporates long-ranged interactions among dislocation segments and misfitting obstacles. The following several sections describe the simulation results and our analysis of their implications. Specifically, we first extract the effective dislocation glide mobility as a function of climb mobility, external stress, obstacle concentration and strength, and dislocation-obstacle interaction range. We then compare the simulation results for the threshold stress to the theoretical predictions outlined above. In the final section, we discuss the implications of our simulation and analytical results, as well as the limitations of the model used in the current study.

II. 2D MODEL OF DISLOCATION MOTION THROUGH A MISFITTING ARRAY OF OBSTACLES

In order to gain insight into the 3D problem, it is useful to consider the simplified problem of the dynamics of straight edge dislocations in the presence of a regular array of cylindrical misfitting obstacles with axes parallel to the dislocation line. We begin with a brief review of some key concepts in dislocation theory. Dislocations are line defects in crystalline materials for which the multivalued elastic displacement vector, $\vec{u}$, satisfies

$$\oint_L d\vec{u} = \vec{b}, \tag{1}$$

where L is any contour enclosing the dislocation line with Burgers vector $\vec{b}$. The Burgers vector, $\vec{b}$, and dislocation line direction, $\vec{\xi}$, can have any orientation with respect to one another. A dislocation for which these vectors are perpendicular (parallel) to each other is an edge (screw) dislocation while the general case is termed a mixed dislocation.

Dislocations migrate in response to stresses in the material, and a commonly used constitutive kinetic law states that dislocation velocities $\vec{v}$ are linearly proportional to the local force on the dislocation line. In short, dislocation dynamics is assumed to be overdamped.[46] More specifically,

$$\vec{v} = \boldsymbol{M} \cdot \vec{f}, \tag{2}$$

where $\boldsymbol{M}$ is the mobility tensor and $\vec{f}$ is the Peach-Koehler force on the dislocation.[47] The mobility tensor for a pure-edge dislocation contains both glide and climb components such that

$$\boldsymbol{M} = m_g(\boldsymbol{I} - \vec{n} \otimes \vec{n}) + m_c \vec{n} \otimes \vec{n}, \tag{3}$$

where $\boldsymbol{I}$ is the unit matrix and the slip plane normal $\vec{n}$ is given by

$$\vec{n} = \frac{\vec{\xi} \times \vec{b}}{|\vec{\xi} \times \vec{b}|}. \tag{4}$$

It should be noted that an atomistic description of dislocation climb would include the mediation of climb by vacancies or interstitials. While a more complete model of climb would contain additional degrees of freedom associated with the dynamics of these point defects, their source/sink nature and diffusion details are often ignored in studies of dislocation dynamics. Finally, the Peach-Koehler force (per unit length) is given by[47]

$$\vec{f} = \boldsymbol{\sigma}_{tot} \cdot (\vec{b} \times \vec{\xi}), \tag{5}$$

where $\boldsymbol{\sigma}_{tot}$ is the total stress that includes the externally applied stress as well as internal stresses due to particles and other dislocations; in the particular case of interest here, $\boldsymbol{\sigma}_{tot} = \boldsymbol{\sigma} + \boldsymbol{\sigma}_{pt}$, where $\boldsymbol{\sigma}$ and $\boldsymbol{\sigma}_{pt}$ denote the applied stress and stress due to the particles, respectively.

We are interested in understanding how the probability of dislocation capture by the obstacles at fixed external stress and glide mobility depends on the climb mobility. Our strategy is to integrate the equation of motion for a straight edge dislocation starting from an arbitrary location relative to an array of misfitting cylindrical particles. In the absence of the particles, the dislocation line would glide in a straight path from, say, right to left. In the current study, the dislocation climb mobility, m_c, ranges from 0 to 1 in units of the dislocation glide mobility, m_g.

A misfitting circular particle generates stress fields both in the matrix and within the particle.[48] More specifically, in Cartesian coordinates, the stress fields for a particle of radius R and eigenstrain ϵ_0 outside the particle $(x^2+y^2>R^2)$ are given by

$$\boldsymbol{\sigma}_{pt} = \frac{PR^2}{2(x^2+y^2)} \begin{pmatrix} \dfrac{-x^2+y^2}{x^2+y^2} & \dfrac{-2xy}{x^2+y^2} \\ \dfrac{-2xy}{x^2+y^2} & \dfrac{x^2-y^2}{x^2+y^2} \end{pmatrix}, \tag{6}$$

while, inside the particle $(x^2+y^2<R^2)$, $\boldsymbol{\sigma}_{pt} = -P\boldsymbol{I}$. In these expressions $P = 4\epsilon_0 G G_0/[2G_0 + G(\kappa_0 - 1)]$, where G is the shear modulus of the matrix and G_0, $\kappa_0 = (\lambda_0 + 3G_0)/(\lambda_0 + G_0)$, $\lambda_0 = 2G_0\nu_0/(1-2\nu_0)$ and ν_0 refer to the shear modulus, bulk modulus, Lamé constant, and Poisson ratio of the particle, respectively.

This model can be employed to study the dynamics of pure-edge dislocations with Burgers vector $\vec{b}=[100]$ and line direction $\vec{\xi}=[001]$, starting at $x=x_0$, $y=y_0$ (where $x_0=3.0$, and y_0 ranges from -3.0 to 3.0, in units of b) in the presence of a misfitting circular particle of radius $R=1.0$ and eigenstrain $\epsilon_0=0.8$ for two different climb mobilities ($m_c=0.1$ and $m_c=1.0$). Under applied shear stress σ_{12} (hereafter abbreviated as σ), edge dislocations move toward the misfitting particle (from right to left) in different fashions, depending upon the magnitude of the applied shear stress and the relative climb and glide mobilities. This is basically a two-dimensional dynamics problem since the pure-edge dislocation under consideration is assumed to always remain straight. In order to focus on the effects of climb and misfit on dislocations bypassing misfitting particles in 2D, we set the elastic constants of the matrix and the particles equal to one another (i.e., we ignore elastic inhomogeneity effects here) and set $\nu = \nu_0 = 0.375$. To be consistent, we use reduced units with b as the unit of length, G as the unit of stress, and m_g as the characteristic mobility scale. We apply periodic

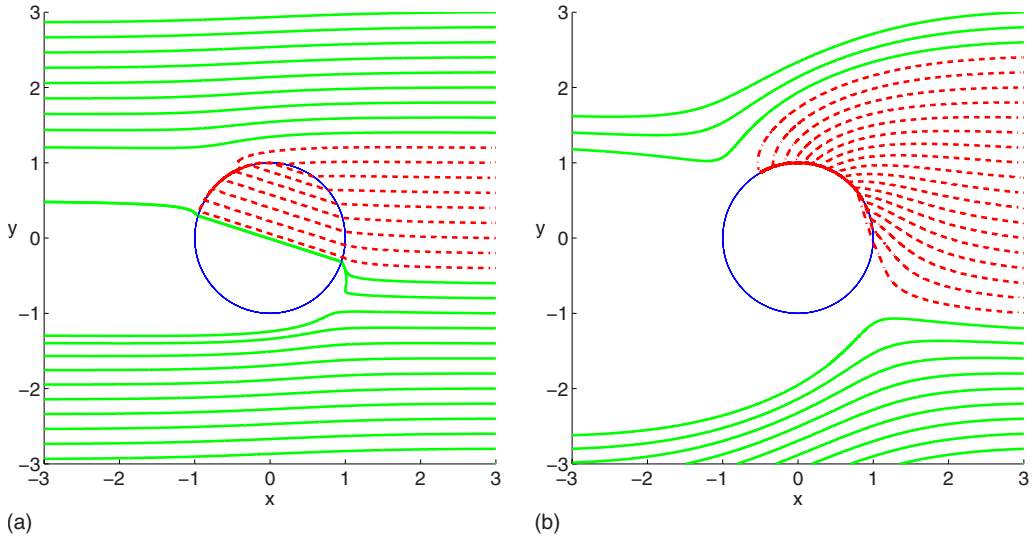

FIG. 1. (Color online) Streamlines starting from $x_0=3.0$, y_0 ranging from −3.0 to 3.0, in presence of a misfitting circular particle of radius $R=1.0$ and misfit strength $f_0=0.8$, for two different climb mobility cases: (a) at a relatively small climb mobility ($m_c=0.1$) and (b) at a large climb mobility ($m_c=1.0$). The dashed streamlines in red denote those edge dislocations pinned by the side of the circular particle though driven by the external shear stress, while the solid streamlines in green refer to edge dislocations able to avoid getting pinned by the particle.

boundary condition along the y axis, and take into account stresses from five periodic images of the circular particle, centered at $(0, kR)$ (where $k=0, \pm 1, \pm 2$).

By monitoring dislocation trajectories for all such initial conditions, one can construct "streamlines" (Fig. 1) for the system, and pinned configurations can be identified as the termini of streamlines that end in the vicinity of the particle. Figures 1(a) and 1(b) display the trajectories of such pure-edge dislocations for two climb mobilities of $m_c=0.1$ and $m_c=1.0$, respectively, at an applied shear stress of $\sigma=-0.4$.

These figures show that, depending upon the initial slip plane of the edge dislocation, the dislocation will either bypass the misfitting particle, cut through it, or become pinned. The red, dashed streamlines denote those edge dislocations pinned on the surface of the circular particle though driven by the external shear stress, while the green, solid streamlines indicate edge dislocations able to traverse the system without getting pinned. More importantly, when the climb mobility increases from 0.1 to 1, the range of initial positions leading to pinning (the dashed streamlines in red) increases substantially, suggesting that in this simple two-dimensional problem greater climb mobility increases the probability of dislocation pinning. Of course, the more interesting, open question is what is the effect of climb on obstacle strengthening in three dimensions, where dislocations can deform and undergo topological changes (loop formations, etc.). As will be discussed below in more detail, the tendency for increased climb mobility increasing the apparent trapping potency of the inclusions in 2D, are borne out by the full 3D simulations.

III. THREE-DIMENSIONAL LEVEL-SET DISLOCATION DYNAMICS METHOD

We use a level-set method first developed by Xiang *et al.*[30] to simulate the motion of an initially straight dislocation, moving under an applied stress, through random arrays of penetrable, misfitting particles. The level-set approach, in this context, can be summarized as follows. A dislocation is represented by the intersection of the zero level sets of two level-set functions, $\phi(\vec{r},t)$ and $\psi(\vec{r},t)$, defined in three-dimensional space such that

$$\phi(\vec{r},t) = \psi(\vec{r},t) = 0. \tag{7}$$

The motion of a dislocation is described then by the time evolution of the level-set functions that satisfy

$$\phi_t + \vec{v} \cdot \nabla \phi = 0, \tag{8}$$

$$\psi_t + \vec{v} \cdot \nabla \psi = 0, \tag{9}$$

where $\vec{v}$ is the velocity field obtained by smoothly extending the velocity of the dislocation to the full three-dimensional space.

The overdamped motion of a dislocation is described by Eq. (2). In general, the mobility can be decomposed into glide and climb components and expressed in tensor form as[30]

$$\boldsymbol{M} = \begin{cases} m_g(\boldsymbol{I} - \vec{n} \otimes \vec{n}) + m_c \vec{n} \otimes \vec{n} & \text{nonscrew}(\vec{\xi} \nparallel \vec{b}) \\ m_g \boldsymbol{I} & \text{screw}(\vec{\xi} \parallel \vec{b}), \end{cases} \tag{10}$$

where $\vec{b}$ is the Burgers vector and the slip plane normal is given by Eq. (4). The Peach-Koehler force per unit length is given by Eq. (5), where $\boldsymbol{\sigma}_{tot}=\boldsymbol{\sigma}_s+\boldsymbol{\sigma}+\boldsymbol{\sigma}_{pt}$ is the total stress that includes contributions from the self-stress $\boldsymbol{\sigma}_s$, external applied stress $\boldsymbol{\sigma}$, and the stresses from the misfitting particles $\boldsymbol{\sigma}_{pt}$.

A misfitting particle generates stresses both in the matrix and within the particle, and the dislocation interacts with these stress fields. In particular, a spherical misfitting particle of radius R embedded in an elastically isotropic medium generates a stress field[49]

$$\boldsymbol{\sigma}_{pt} = \frac{2G\epsilon R^3}{r^5}(r^2\boldsymbol{I} - 3\vec{r}\otimes\vec{r})\Theta(r-R) - 4G\epsilon\boldsymbol{I}\Theta(R-r), \tag{11}$$

where r denotes the distance from the point to the particle center, $\epsilon = \epsilon_0(1+\nu)/[3(1-\nu)]$, ϵ_0 is the dilatational misfit strain and Θ denotes a step function with $\Theta(x)=1$ for $x>0$ and $\Theta(x)=0$ otherwise. We note that ϵ controls the strength of the dislocation-obstacle force.

In our simulations, the elasticity equations associated with the dislocations are solved using a standard fast Fourier-transform approach with periodic boundary conditions.[30,50] The level-set evolution equations are solved using the third-order weighted essentially nonoscillatory method[51] for the spatial discretization and a fourth-order total variation diminishing Runge-Kutta technique for the temporal evolution.[52] As is customary, the simulation results are reported in nondimensional forms, where all lengths are normalized by b, energies by Gb^3 and dislocation mobilities by m_g.

The three-dimensional level-set method has been applied to study dislocation-particle bypass mechanisms[31,32] in a variety of cases, including penetrable or impenetrable, misfitting or nonmisfitting particles, with or without climb. These investigations have revealed several different mechanism by which dislocations bypass spherical particles, including particle cutting, many different forms of dislocation loop formation and combinations of these mechanisms.

A brief summary of the results of Xiang *et al.*[31,32] sets the stage for this work. Most significantly, they find that, depending on the relative position of the initial slip plane and the center of the misfitting particle, allowing climb can either increase or decrease the critical stress for an initially straight edge dislocation to bypass a regular array of particles. For example, climb can facilitate obstacle bypass by providing an alternative path around the obstacle with an attendant decrease in the critical stress. By contrast, if the initial slip plane of the edge dislocation intersects the particle center, in the absence of climb there is no glide force generated by the misfitting particle due to symmetry, and so the dislocation simply cuts through the particle.[32] When the climb mobility is appreciable, at small applied stresses, the dislocation is pinned by the particle and a prismatic loop is formed. In this latter case, climb motion allows the dislocation to reach a more stable, pinned configuration than that without climb, and therefore the critical stress increases. Thus, whether dislocation climb facilitates bypassing or hinders it in the regular array case depends on the initial condition. This is similar to its two-dimensional analogy as analyzed in Sec. II, which led to the conclusion that higher climb mobility results in a greater likelihood that an edge dislocation, starting from an arbitrary initial position, will get pinned by the misfitting particles under the same applied shear stress. Naturally, it is of interest to investigate next whether climb leads statistically to more or less effective pinning by randomly distributed obstacles.

IV. DISLOCATION MOTION IN A 3D FIELD OF RANDOMLY DISTRIBUTED OBSTACLES

As indicated above, an extended defect may be deflected from its nominal plane of propagation by an encounter with an obstacle. For example, crack deflection that results in toughening can occur in the presence of reinforcing obstacles in composites where local stresses will affect the deflection process.[12,53] Our overdamped dislocation model provides a convenient example of out-of-plane motion of an extended defect. Having examined the impact of climb on obstacle bypass in an idealized, quasi-two-dimensional situation in Sec. II and summarized dislocation bypass of a regular array of spherical particles in three dimensions, we therefore investigate the evolution of an edge dislocation as it moves through a field of randomly distributed misfitting obstacles in three dimensions using the level-set method for dislocation dynamics.

For concreteness, the initial configuration is taken to be a straight edge dislocation with Burgers vector $\vec{b}=[010]$ and line direction $\vec{\xi}=[001]$ and the applied shear stress is σ_{12} (hereafter referred to as σ). The dislocation core radius is $\epsilon_c=3$ and the computational domain has dimensions $30\times30\times60$ discretized onto a grid of size $32\times32\times64$. Statistically meaningful results are obtained for each set of physical parameters by averaging over 90 different, randomly generated initial particle configurations for an obstacle concentration of $c=0.0093$ and a misfit strength of $f_0=2.0$ (these parameters are varied below in order to explore the impact of obstacle concentration and misfit strength on dislocation motion). We begin with a qualitative description of dislocation motion in the different kinematic regimes.

For dislocations with low-climb mobility (e.g., $m_c=0.1$), dislocation motion is in one of three regimes depending upon the magnitude of the applied shear stress. When σ is sufficiently small, the dislocation initially moves slowly in its glide plane, but has ample opportunity to climb as it approaches a particle, and eventually becomes pinned. Figure 2 illustrates this first regime of dislocation motion for $\sigma=0.1$. (Note that in all of the simulation images shown below, the colors are indexed according to the x coordinate, i.e., the displacement away from the initial glide plane.) By contrast, at an intermediate stress (above the critical stress) $\sigma=0.5>\sigma_c$, both dislocation pinning and depinning are observed. From an analysis of simulation images (see Fig. 3), it is evident that this process occurs via the bowing of the dislocation until the associated line tension increases to a level permitting break away and, in some cases, the formation of prismatic loops. As a result, the dislocation advances with a relatively small average velocity. Since the rate of dislocation advance is constant (apart from statistical fluctuations), we are able to determine a nonzero, effective dislocation glide mobility (see below). Finally, when the applied shear stress is much higher, the dislocation moves along the initial glide plane sufficiently rapidly such that there is little oppor-

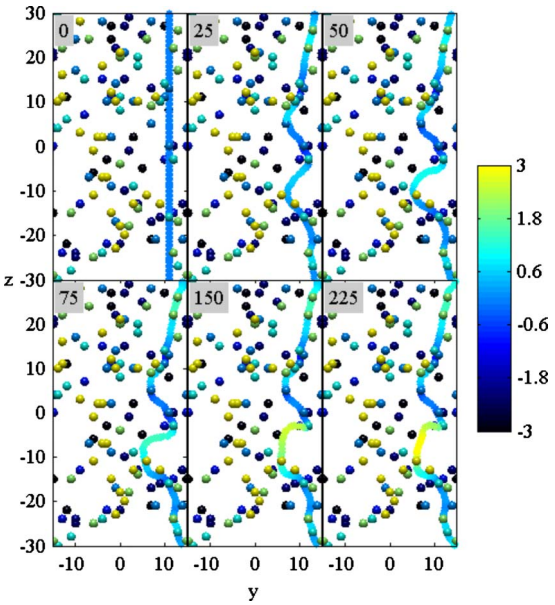

FIG. 2. (Color online) Simulation of the motion of a dislocation line with a low-climb mobility (m_c=0.1) subject to a small applied stress (σ=0.1). Note that the climb displacement is only a few lattice spacings. The color indicates the position of the dislocation and particles in the x direction (i.e., normal to the slip plane).

tunity for it to explore out-of-plane pinning sites. Figure 4 illustrates this high-velocity regime. It should be noted that in this regime, the dislocation line remains nearly straight as it advances (as expected).

For dislocations with high-climb mobility (e.g., m_c=1.0), on the other hand, the propensity for climb alters the critical applied shear stress, as discussed below. At low applied stresses (e.g., σ=0.1), the dislocation initially moves very

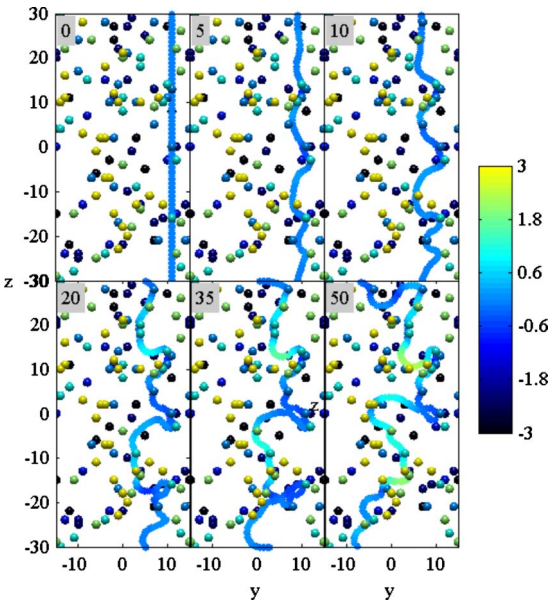

FIG. 3. (Color online) Simulation of the motion of a dislocation line with a low-climb mobility (m_c=0.1) under an intermediate applied stress (σ=0.5). The dislocation glides with a relatively small average velocity.

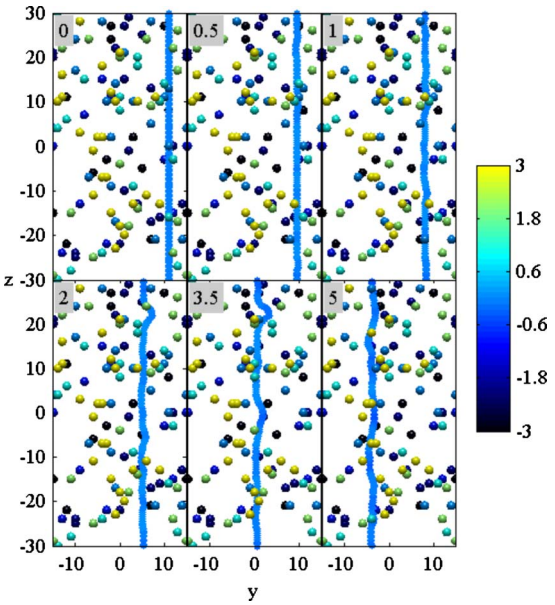

FIG. 4. (Color online) Simulation of the motion of a dislocation line with a low-climb mobility (m_c=0.1) under high applied stress (σ=3.0). Little pinning occurs, and there is also no appreciable climb.

slowly on its glide plane but readily climbs out of the glide plane resulting in more extensive pinning by obstacles. Similar to what is observed in the low-climb regime, local unpinning leads to remnant dislocation loops decorating the particles. On the other hand, at an intermediate shear stress (σ=0.5), which is now below the critical stress (σ_c=0.52), climb is more extensive, and the dislocation explores more pinning centers in three-dimensional space as segments are locally pinned. As a result, the dislocation lines becomes markedly rougher, leading to local unpinning. Finally, in the high stress regime (σ=3.0), dislocation motion is similar to that observed in the corresponding low-climb mobility (m_c=0.1) limit, i.e., the dislocation moves along its glide plane, relatively unperturbed by obstacles.

The physical picture that emerges from these observations is as follows. For an arbitrary climb mobility, a dislocation moving in a field of randomly distributed obstacles gets pinned by the particles when the stress is lower than the threshold stress. As the applied stress increases toward the threshold stress, some parts of the dislocation depin from the particles while other parts remain pinned, leading to complex spatiotemporal dynamics. Finally, when the external stress is sufficiently large, the motion of the dislocation line is only slightly perturbed by the obstacles. We quantify the dependence of the threshold stress on dislocation climb, obstacle strength, obstacle concentration, and dislocation-obstacle interaction range below.

The simulation results indicate that dislocation motion is retarded by elastic interactions between the obstacles and the dislocation. While one might expect that climb facilitates motion through the obstacles, the simulation results presented above indicate that an increase in climb mobility makes dislocation motion more difficult, increasing the threshold stress. It is worth noting, as pointed out by

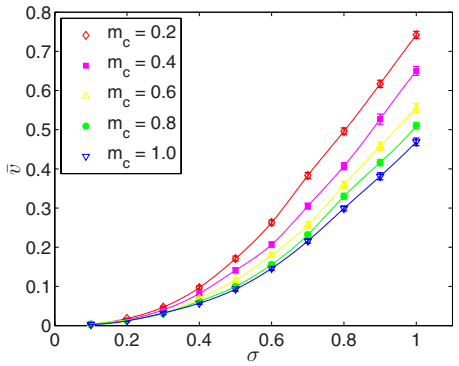

FIG. 5. (Color online) The average speed, $\bar{v}$, of the center of mass of the dislocation as a function of applied shear stress for various climb mobilities (m_c=0.2, 0.4, 0.6, 0.8, and 1.0). The error bars are determined from the results of 90 independent simulations in which the obstacles are randomly distributed. Note the decrease in $\bar{v}$ upon increasing m_c.

Xiang,[32] that the numerical methods used in the present simulations do not completely prevent the motion of dislocations out of their slip plane even when the climb mobility is set to zero. This type of "numerical climb" is very slow and is equivalent to having a very small climb mobility. So, in the current study, the smallest climb mobility we employ in our investigation of the effect of climb on obstacle strengthening is much larger that this numerical climb mobility.

Next, we examine the dislocation motion more quantitatively by considering the average speed of the center of mass of the dislocation line along the initial glide plane, $\bar{v}$, as a function of σ for several values of the climb mobility m_c (see Fig. 5). First, we note that the dislocation velocity is a nonlinear, monotonically increasing function of applied stress, even though the fundamental equation of motion for the dislocation, Eq. (2), is linear. This suggests that the common observation that *macroscopic* dislocation velocity-stress relations are nonlinear, increasing functions of stress when dislocation motion is overdamped may, under some circumstances, be the result of dislocations bypassing obstacles. Upon increasing m_c, the $\bar{v}$ versus σ curve shifts downwards, indicating that the effective glide mobility of the dislocation is reduced. Moreover, as will be seen below, the threshold stress increases with increasing m_c. A major conclusion of this work is that dislocation climb in the presence of a field of penetrable obstacles retards dislocation motion.

Dislocation conformations also depend upon the applied stress σ and the climb mobility m_c. This dependence may be quantified in terms of the out-of-plane and in-plane dislocation roughnesses. The out-of-plane dislocation roughness (i.e., perpendicular to the nominal glide plane), $W_\perp$, is defined as the excess dislocation line length when projected onto the xz plane, i.e., $W_\perp=(l_\perp-l_0)/l_0$, where l_0 is the original dislocation length and $l_\perp$ is the dislocation length when projected onto the xz plane. In a similar manner, the in-plane dislocation roughness is $W_\parallel=(l_\parallel-l_0)/l_0$, where $l_\parallel$ is the dislocation length when projected onto the glide (yz) plane. $W_\perp$ and $W_\parallel$ are plotted as a function of σ for several m_c in Figs. 6 and 7, respectively. There are two key observations: first,

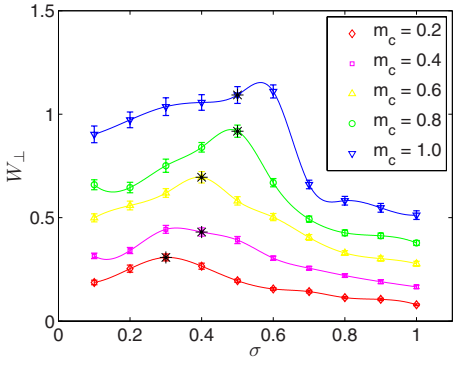

FIG. 6. (Color online) Plot of out-of-plane dislocation roughness $W_\perp$ as a function of applied shear stress σ at different dislocation climb mobilities (m_c=0.2, 0.4, 0.6, 0.8, and 1.0).

both $W_\perp$ and $W_\parallel$ display a nonmonotonic dependence on σ, with a maximum in the vicinity of the threshold stress σ_c. Second, both $W_\perp$ and $W_\parallel$ increase with increasing m_c at fixed σ, given the additional free volume (the potential volume that a dislocation can explore in the three-dimensional space) associated with climb.

We can define the threshold stress, σ_c, as the stress at which the dislocation overcomes the retarding effect of the surrounding obstacles and can move through the entire obstacles field. In practice, we define σ_c through the slope of the velocity-stress curve as follows:

$$\left.\frac{d\bar{v}}{d\sigma}\right|_{\sigma=\sigma_c}=\frac{1}{2}. \tag{12}$$

The σ_c values, obtained in this manner, coincide with the stress values at which the two roughness values reach their respective maxima. In practice, σ_c are located by first fitting the $\bar{v}$ vs σ curves to a polynomial and then evaluating Eq. (12) analytically.

Figure 8 shows σ_c versus m_c for several obstacle concentrations and misfit strengths. As can be seen, σ_c is a linear function of m_c. This is illustrated most clearly for an obstacle concentration of c=0.0093 and a misfit strength of f_0=2.0. Not surprisingly, the magnitude of the obstacle strengthening

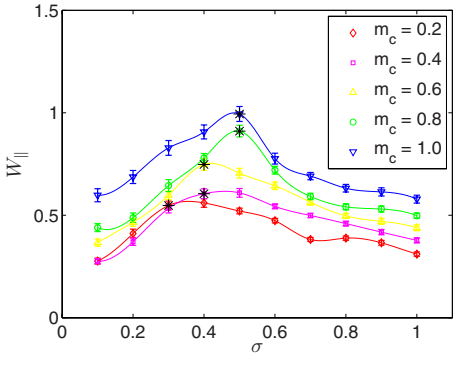

FIG. 7. (Color online) Plot of in-plane dislocation roughness $W_\parallel$ as a function of applied shear stress σ at different dislocation climb mobilities (m_c=0.2, 0.4, 0.6, 0.8, and 1.0).

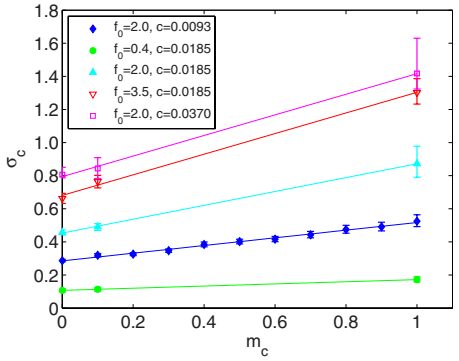

FIG. 8. (Color online) Plot of critical applied shear stress σ_c as a function of dislocation climb mobility m_c with different obstacle concentration and misfit strength.

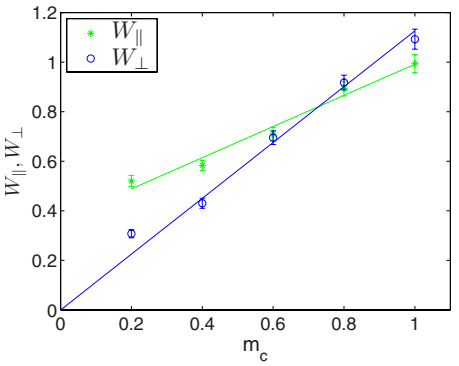

FIG. 10. (Color online) Dislocation in-plane and out-of-plane roughness near critical applied shear stress σ_c at different dislocation climb mobilities m_c.

effect increases with increasing obstacle concentration and misfit.

We can also define a stress-dependent, effective dislocation glide mobility, $m_g^*(\sigma)$, from the relation $\bar{v} \equiv m_g^*(\sigma)\sigma$. Obviously, m_g^* is a function of obstacle concentration, spatial distribution, and misfit, and of the dislocation climb mobility and applied stress. Figure 9 shows m_g^* as a function of σ for five different climb mobilities. The data show that the effective dislocation glide mobility decreases with increasing climb mobility, m_c, as anticipated above.

Finally, we address the dependence of σ_c on obstacle concentration and strength. We have performed simulations with obstacle concentrations $c=0.0185$ and 0.0370 with fixed particle misfit strength $f_0=2$, and two different misfit strengths, $f_0=0.4$ and 3.5 at fixed particle concentration $c=0.0185$.

Three climb mobilities were considered, namely, $m_c=0$, 0.1, and 1 for all these cases. The threshold stress versus climb mobility for different particle concentrations and misfit strengths is plotted in Fig. 8. Again, an approximate linear dependence of the (reduced) threshold stress on climb mobility is observed.

V. DISCUSSION

The increase in obstacle hardening with dislocation climb, a seemingly counterintuitive phenomenon, can be best understood by considering the following effects from a statistical perspective. On the one hand, the simple 2D view as detailed in Sec. II suggests that with increasing climb mobility, it is statistically more probable for dislocations to get pinned by the penetrable misfitting obstacles, even in the absence of an applied stress. On the other hand, since dislocations are capable of exploring energy landscapes in three dimensions, the effect of climb on dislocation conformations near pinning can be relevant. Intuitively, an increase in the climb mobility allows the dislocation line to explore nearby pinning centers more effectively. To quantify this effect, we plotted $W_\perp$ and $W_\parallel$ near σ_c as a function of m_c in Fig. 10. The out-of-plane roughness $W_\perp$ at threshold increases much more with increasing m_c than does the in-plane roughness $W_\parallel$. In other words, increasing the climb mobility allows the dislocation line to explore a wider range of local pinning sites, leading to both increased out-of-plane roughness and more effective pinning. Statistically, the number of pinning sites N a dislocation can explore is proportional to the volume it occupies: $N \sim cLR^2$, where $L \approx l_0(1+W_\perp+W_\parallel)$ is the total dislocation length. Also note that at threshold, $W_\perp \propto m_c$ and $W_\parallel \propto m_c$ (cf. Fig. 10), implying that L has a linear dependence on the climb mobility. This implies that the threshold stress has a similar linear dependence on m_c. It is worthwhile to note that this is different from the classical Orowan mechanism by which an edge dislocation bypasses an array of obstacles that are impermeable to dislocations. Xiang *et al.*[30] modeled the Orowan process by assuming that the obstacles exert only very short-ranged repulsive forces on the dislocation. In that case, dislocation motion will be blocked by the obstacles unless climb or cross slip occurs. In other words, climb provides additional degrees of freedom by which dislocations can overcome the energetic barriers associated with the obstacles, and therefore facilitates dislocation bypassing obstacles if the obstacles are impenetrable (as opposed to the long-ranged elastic interactions between misfitting, penetrable obstacles considered here).

To explore the extent to which the climb-strengthening effect depends on the long-ranged nature of the interactions between the dislocation and penetrable misfitting obstacles, the stress field is further modulated with an exponentially decaying factor such that the stress field outside the misfitting particle now becomes

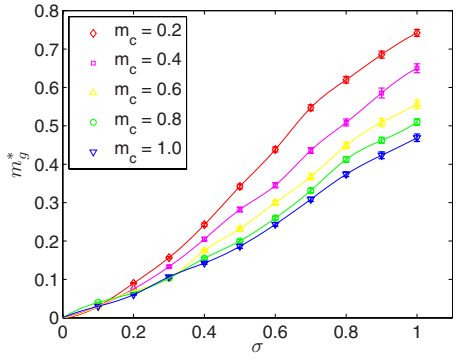

FIG. 9. (Color online) The dislocation effective glide mobility as a function of external applied shear stress at different climb mobilities (m_c=0.2, 0.4, 0.6, 0.8, and 1.0).

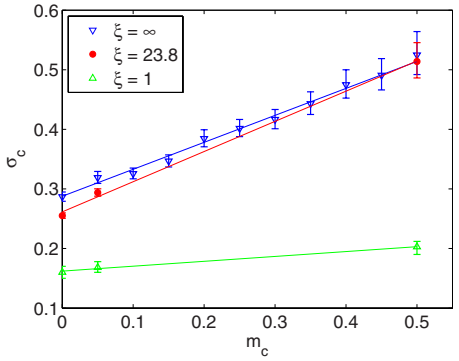

FIG. 11. (Color online) Critical applied shear stress σ_c as a function of climb mobility m_c with different decay lengths ($\xi=\infty$, 23.8, and 1).

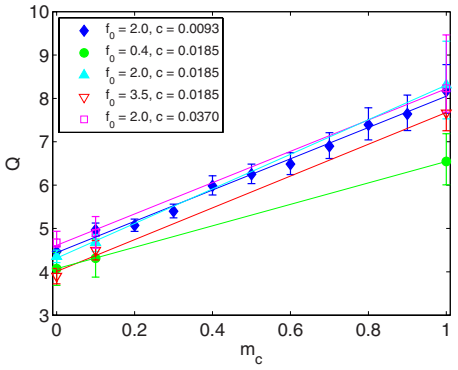

FIG. 12. (Color online) Reduced critical applied shear stress ($Q=\sigma_c/f_0^\alpha c^\beta$) as a function of climb mobility m_c with different sets of obstacle concentration and misfit strength.

$$\boldsymbol{\sigma}_{pt}^{*} = \boldsymbol{\sigma}_{pt} \exp\left(-\frac{|r-R|}{\xi}\right), \tag{13}$$

where $\boldsymbol{\sigma}_{pt}$ is defined in Eq. (11) and ξ is an effective interaction length (the stress field inside the particle is unmodified). Thus, setting $\xi=\infty$ corresponds to the case described above, featuring long-ranged dislocation-obstacle interactions, while a finite ξ implies short-ranged dislocation-obstacle interactions. The phenomenological interaction in Eq. (13) allows us to conveniently tune the range of the dislocation-obstacle interaction while keeping the maximum interaction (i.e., pinning) force at $r=R$ fixed. We also note that the presence of such short-ranged interactions is usually assumed in important driven systems, such as pinning of flux lines and flux-line lattices.[2]

Figure 11 shows the critical stress σ_c as a function of climb mobility for three different interaction lengths $\xi=\infty$, $5c^{-1/3}\approx 23.8$, and 1. In all cases, the threshold stress increases approximately linearly with climb mobility. When $\xi=23.8$, corresponding to five times the average obstacle spacing, the critical stresses at $m_c=0$, 0.1, and 1 are very close to the long-ranged ($\xi=\infty$) case. However, when the interaction length is reduced to the order of a grid spacing (i.e., $\xi=1$), the threshold stresses become much smaller, yet still scale linearly with climb mobility, albeit with a smaller slope. Thus, the strengthening due to increased climb mobility is amplified by long-ranged dislocation-obstacle interactions.

As reviewed in Sec. I, several different theoretical models[21,40,44,54] predict a power-law relation between the critical stress and the particle misfit and concentration. To test these predictions, we have attempted to collapse the data in Fig. 8 through the following procedure. By assuming that the threshold stress can be described as $\sigma_c \sim f_0^\alpha c^\beta h(m_c)$, where $h(m_c)=a+bm_c$, a proper choice of α and β would collapse the $Q=\sigma_c/(f_0^\alpha c^\beta)$ versus m_c data onto a single universal curve. It is worthwhile to point out that in the models as reviewed in Sec. I, the concentration c_0 refers to the atomic density per unit area on the slip plane. The relationship between c_0 and the volume concentration c we use is given by $c_0=c^{2/3}$. The best data collapse for our limited data, shown in Fig. 12, is obtained for $\alpha=0.86$ and $\beta=0.71$, i.e., $\sigma_c \propto f_0^\alpha c^{0.71}=f_0^\alpha c_0^{1.07}$. The best agreement between this result and the existing models is for the Friedel-Suzuki theory, which predicts that $\sigma_c \propto f_0 c_0$. A simple way to understand the appearance of such a low value of α is to consider the limit $f_0 \to \infty$ in which an elastic string would require an infinite external stress to depin, while a dislocation line, capable of forming loops, depins at a finite stress (which depends on dislocation line tension and distance between pinning sites). In other words, in this limit, σ_c is independent of f_0, and loop formation dominates depinning. While it is tempting to argue that our data correspond to a situation where both looping and classical depinning contribute to the observed behavior, alternative models of complex pinning phenomena that are beyond the scope of the present paper, are required in order to fully explain these results.

Given the important role of dislocation climb on strengthening by penetrable obstacles discussed above, it is worthwhile to review both the physical mechanisms which facilitate dislocation climb and how these mechanisms are usually incorporated in dislocation dynamics simulations. Dislocation climb involves diffusion of interstitials or vacancies and has a strong temperature dependence. Given its importance in dislocation motion, there have been extensive theoretical studies of interstitial and vacancy-mediated dislocation climb mechanisms.[31,32,55–60] For example, Reynolds *et al.*[57] developed a model for the motion of a pinned dislocation climbing under an external stress by assuming that the climb velocity is linearly dependent on the climb force. Amodeo and Ghoniem[58] also assumed that the climb rate is proportional to the climb force based on the phenomenological expression for the dislocation climb rate given by Argon *et al.*[9] The same assumption was adopted in the two-dimensional DD technique developed by Roters *et al.*[60] but with a different proportionality factor between climb rate and climb force. More recently, Mordehai *et al.*[55] proposed a method for discrete dislocation dynamics in which dislocation climb by bulk diffusion was introduced. In their model, by assuming that at each time step the vacancy flux is in steady state and neglecting the elastic interaction energy between dislocations and vacancies, they found that the climb rate dependence on mechanical climb force was

$$\vec{v}_{cl} \propto \left(e^{F_{cl}\Omega/bkT} - \frac{C_\infty}{C_0} \right) \vec{n}, \tag{14}$$

where F_{cl} is the mechanical climb force, Ω is an atomic volume, $\vec{n}$ is the unit vector in the climb direction, C_∞ is the average vacancy concentration in the bulk, and C_0 refers to the equilibrium vacancy concentration in a defect-free crystal.

In our continuum DD method, we adopted the computational approach of Xiang *et al.*;[30] treating dislocation motion as overdamped, i.e., dislocation velocities are linearly proportional to the local stresses,[46] and the proportionality is controlled by the local mobility tensor that includes both glide and climb components.[30] Although diffusion of atoms or vacancies is not explicitly treated in this approach, it is implicitly incorporated in the atomistically informed, local mobility tensor. We note that this method could be equivalent to Mordehai's model in the regime where the climb force is relatively small and assuming a uniform vacancy distribution outside the dislocation core region ($c_\infty = c_0$) such that the climb rate is directly proportional to the mechanical climb force ($\vec{v}_{cl} \propto \vec{F}_{cl}$) in the first-order approximation. As indicated earlier, this level-set method for dislocation dynamics has been successfully used to demonstrate the shrinkage of circular prismatic loops[30] and to explore the bypass mechanisms of an edge dislocation over an obstacle via climb.[31,32]

At this point, it is important to recall some of the limitations of the current simulation approach. Although the level-set method for DD has the advantage over discrete atomistic methods in the sense that it can be used to simulate a relatively large volume of material (an advantage it shares with other continuum methods), it accounts for the atomistic discreteness of the crystalline lattice in a very simplified manner. The Burgers vectors are determined by the discreteness and periodicity of the lattice, yet all information about the structure and dynamics of the dislocation core is captured in a single composite quantity, the dislocation mobility. While the dislocation glide mobility may be controlled by interaction of the dislocations with phonons, the dynamics of double kink nucleation, and the nature of the Peierls barrier, in the present simulations, all of these effects are combined into the single, coarse-grained parameter, m_g. While the dislocation climb mobility may be controlled by the ease of formation or annihilation of vacancies or interstitials (point defects) in the dislocation core and the diffusion of point defects between dislocations or dislocation segments, all of these effects are again combined into the single, coarse-grained parameter, m_c. Coarse-graining procedures necessarily combine many important atomistic processes into a small number of effective parameters and inevitably omit details that may be important in certain regimes. Nonetheless, such approaches are necessary in describing phenomena on temporal and spatial scales that are too large to include all atomistic details. The important question in all coarse-graining approaches is, "does the coarse graining wipe out details that are central to the questions being asked?" The focus of the present study is to answer the question, "how does dislocation motion out of the glide plane (particularly by dislocation climb) modify the plastic flow behavior in systems containing randomly distributed, stationary obstacles?"

The assumption of constant climb mobility, implies the dislocations are effective point-defect source and/or sinks and that long-range diffusion is not necessary. While the first condition is a common assumption, the latter applies under a more restrictive set of conditions. For example, it applies in cases where there is a supersaturation of point defects. Such conditions are common in materials undergoing significant plastic deformation or under irradiation. If long-range diffusion is necessary, the coupling of dislocation climb to the dynamic point-defect field may be important. In this regime, the approach of Mordehai *et al.*,[55] which incorporates point-defect diffusion, is perhaps more realistic, although their use of an edge-screw discretization of the dislocation line and their neglect of glide and cross slip seriously limits its applicability.

In the present study, the assumption of constant climb mobility is consistent with the focus on the effect of climb on the three-dimensional nature of dislocation motion through a field of obstacles. Including long-range diffusion and point-defect adsorption and formation will surely modify the details of dislocation motion but will not change the main features of the simulations, i.e., climb allows for edge dislocation motion off the initial glide plane. The magnitude of the dislocation climb mobility is, on the other hand, sensitive to this level of description of the point-defect dynamics. Therefore, trying to pin a climb mobility value for a real material under specified conditions (e.g., temperature and stress) is very complicated. Because our focus was on evaluating the effect of climb, we chose an approach in which climb is a parameter that is varied to clarify the effect (rather than model a particular set of physical conditions). In order to make the effect of climb very evident, we also chose larger values for the climb mobility than is commonly observed in metallurgical samples. Of course, should such a mapping from point-defect densities and mobilities to coarse-grained dislocation mobilities become available via, e.g., more microscopic simulations specific to a particular system of interest, the level-set formalism employed in this paper provides a convenient means to quantitatively simulate the response of both isolated dislocations and collections thereof under stress.

With the aforementioned caveats in mind, the present model provides insight into the transverse motion of extended defects as they encounter obstacles in systems with long-ranged interactions. As our illustration of defect motion is dislocation dynamics in the presence of obstacles, we have also begun to lay the groundwork for a multiscale modeling approach to plasticity. In this more general framework for plasticity, first solutal and point-defect degrees of freedom are integrated out and subsumed into an effective mobility tensor, and then dislocation ensembles consisting of collections of individual dislocation lines are coarse grained into spatially dependent dislocation densities. Physically based, closed-form kinetic equations for the dislocation densities may ultimately provide a means to derive microscopically informed constitutive laws for the mesoscale.

VI. CONCLUSIONS

In this paper, we presented the results of a three-dimensional level-set simulation of dislocation motion

through an array of stationary, penetrable, misfitting obstacles as an illustration of the role of out-of-plane motion on the pinning-depinning behavior of mobile, extended objects. Specifically, the effects of dislocation climb, obstacle concentration and strength, and the range of dislocation-obstacle interactions on threshold stress were quantified. Most significantly, we demonstrated that allowing climb can lead to more effective dislocation pinning. This counterintuitive result can be understood by noting that climb allows the dislocation to explore a larger obstacle neighborhood to find more effective pinning sites (deeper energy wells). Decreasing the interaction range significantly diminishes this effect. We also explored the scaling of the threshold stress with obstacle concentration and misfit strength, and found that our results are in reasonable agreement with the theory of Friedel[21] and Suzuki.[44] Because the simulation approach applied herein focuses on a coarse-grained description of the glide and climb of dislocations, its ability to mimic the behavior of any specific material or set of conditions is limited.

In broader terms, the work described here may be incorporated within a multiscale modeling approach to plasticity, wherein first solutal and point-defect degrees of freedom are integrated out and subsumed into an effective glide mobility, and then dislocation ensembles consisting of collections of individual dislocation lines are coarse grained into spatially dependent dislocation densities. The dynamics of these dislocation densities may then be employed to construct phenomenological, microscopically informed constitutive laws appropriate for the mesoscale.

ACKNOWLEDGMENTS

The authors would like to thank the Air Force Office of Scientific Research for support under Grant No. FA9550-05-1-0082. This work has also been supported in part by an NSF-DMR under Grant No. 0449184 (M.H.).

[1] D. Ertas and M. Kardar, Phys. Rev. B **53**, 3520 (1996).
[2] G. Blatter, M. V. Feigel'man, V. B. Geshkenbein, A. I. Larkin, and V. M. Vinokur, Rev. Mod. Phys. **66**, 1125 (1994).
[3] S. Lemerle, J. Ferré, C. Chappert, V. Mathet, T. Giamarchi, and P. Le Doussal, Phys. Rev. Lett. **80**, 849 (1998).
[4] T. Tybell, P. Paruch, T. Giamarchi, and J. M. Triscone, Phys. Rev. Lett. **89**, 097601 (2002).
[5] G. Grüner, Rev. Mod. Phys. **60**, 1129 (1988).
[6] P. G. de Gennes, Rev. Mod. Phys. **57**, 827 (1985).
[7] S. Ramanathan, D. Ertas, and D. S. Fisher, Phys. Rev. Lett. **79**, 873 (1997).
[8] B. Wetzel, P. Rosso, F. Haupert, and K. Friedrich, Eng. Fract. Mech. **73**, 2375 (2006).
[9] W. Scholz, J. Fidler, T. Schrefl, D. Suess, and T. Matthias, J. Appl. Phys. **91**, 8492 (2002).
[10] J. Lefebvre, M. Hilke, R. Gagnon, and Z. Altounian, Phys. Rev. B **74**, 174509 (2006).
[11] G. P. Mikitik and E. H. Brandt, Phys. Rev. B **79**, 020506(R) (2009).
[12] D. J. Green, *An Introduction to the Mechanical Properties of Ceramics* (Cambridge University Press, Cambridge, 1998).
[13] D. C. Chrzan and M. S. Daw, Phys. Rev. B **55**, 798 (1997).
[14] S. Zapperi and M. Zaiser, Mater. Sci. Eng., A **309-310**, 348 (2001).
[15] J. P. Hirth and J. Lothe, *Theory of Dislocations*, 2nd ed. (Krieger, Malabar, Florida, 1992).
[16] D. Y. Seo, J. Beddoes, L. Zhao, and G. Botton, Mater. Sci. Eng., A **329-331**, 810 (2002).
[17] P. R. Subramanian, M. G. Mendiratta, D. M. Dimiduk, and M. A. Stucke, Mater. Sci. Eng., A **239-240**, 1 (1997).
[18] L. Reich, M. Murayama, and K. Hono, Acta Mater. **46**, 6053 (1998).
[19] S. P. Ringer, T. Sakurai, and I. J. Polmear, Acta Mater. **45**, 3731 (1997).
[20] P. S. Tantri, A. K. Bhattacharya, and S. K. Ramasesha, Proc. Indian Acad. Sci. (Chem. Sci.) **113**, 633 (2001).
[21] J. Friedel, *Dislocations* (Pergamon, New York, 1964).
[22] A. A. Benzerga, Y. Bréchet, A. Needleman, and E. Van Der Giessen, Modell. Simul. Mater. Sci. Eng. **12**, 159 (2004).
[23] L. P. Kubin and G. R. Canova, in *Electron Microscopy in Plasticity and Fracture Research of Materials*, edited by U. Messerschmidt, F. Appel, J. Heydenreich, and V. Schmidt (Akademie Verlag, Berlin, 1990), p. 23.
[24] L. P. Kubin, G. Canova, M. Condat, B. Devincre, V. Pontikis, and Y. Brechet, Solid State Phenom. **23-24**, 455 (1992).
[25] H. M. Zbib, M. Rhee, and J. P. Hirth, Int. J. Mech. Sci. **40**, 113 (1998).
[26] M. Rhee, H. M. Zbib, J. P. Hirth, H. Huang, and T. de laRubia, Modell. Simul. Mater. Sci. Eng. **6**, 467 (1998).
[27] K. W. Schwarz, J. Appl. Phys. **85**, 108 (1999).
[28] Y. Wang, D. J. Srolovitz, J. M. Rickman, and R. LeSar, Acta Mater. **48**, 2163 (2000).
[29] J. M. Rickman, M. P. Haataja, and R. LeSar, Phys. Rev. B **77**, 174105 (2008).
[30] Y. Xiang, L. T. Cheng, D. J. Srolovitz, and W. E., Acta Mater. **51**, 5499 (2003).
[31] Y. Xiang, D. J. Srolovitz, L. T. Cheng, and W. E., Acta Mater. **52**, 1745 (2004).
[32] Y. Xiang and D. J. Srolovitz, Philos. Mag. **86**, 3937 (2006).
[33] A. D. Brailsford, Phys. Rev. **139**, A1813 (1965).
[34] M. Dong, M. C. Marchetti, A. A. Middleton, and V. Vinokur, Phys. Rev. Lett. **70**, 662 (1993).
[35] A. Foreman and M. Makin, Philos. Mag. **14**, 911 (1966).
[36] T. Nogaret and D. Rodney, Phys. Rev. B **74**, 134110 (2006).
[37] M. Z. Butt and P. Feltham, J. Mater. Sci. **28**, 2557 (1993).
[38] H. Neuhäuser, Phys. Scr. T **49**, 412 (1993).
[39] N. F. Mott and R. N. Nabarro, Proc. Phys. Soc. London **52**, 86 (1940); *Report of a Conference on the Strength of Solids* (The Physical Society, London, 1948).
[40] R. Labusch, Phys. Status Solidi **41**, 659 (1970).
[41] R. Labusch, Acta Metall. **20**, 917 (1972).
[42] Z. Trojanová, P. Vostry, and J. Maisnar, Czech. J. Phys., Sect. B **B28**, 113 (1978).
[43] R. N. Nabarro, Philos. Mag. **35**, 613 (1977).

[44] T. Suzuki, S. Takeuchi, and H. Yoshinaga, *Dislocation Dynamics and Plasticity* (Springer-Verlag, Berlin, 1991), p. 32.
[45] S. Patinet and L. Proville, Phys. Rev. B **78**, 104109 (2008).
[46] M. Carmen Miguel, A. Vespignani, M. Zaiser, and S. Zapperi, Phys. Rev. Lett. **89**, 165501 (2002).
[47] M. Peach and J. S. Koehler, Phys. Rev. **80**, 436 (1950).
[48] N. I. Muskhelishvili, *Some Basic Problems of The Mathematical Theory of Elasticity* (Noordhoff, Groningen, 1963), p. 216.
[49] J. D. Eshelby, in *Solid State Physics*, edited by F. Seitz and D. Turnbull (Academic, New York, 1956), Vol. 3.
[50] V. V. Bulatov, M. Rhee, and W. Cai, in *Multiscale Modeling of Materials–2000*, edited by L. Kubin, J. L. Bassani, K. Cho, H. Gao, and R. L. B. Selinger (Materials Research Society, Warrendale, PA, 2001).
[51] G. S. Jiang and D. Peng, SIAM J. Sci. Comput. (USA) **21**, 2126 (2000).
[52] R. J. Spiteri and S. J. Ruuth, SIAM (Soc. Ind. Appl. Math.) J. Numer. Anal. **40**, 469 (2002).
[53] S. Suresh, *Fatigue of Materials* (Cambridge University Press, Cambridge, 1998).
[54] R. L. Fleischer and W. R. Hibbard, *The Relation of Structure to Mechanical Properties of Metals* (Her Majesty's Stationary Office, London, 1963).
[55] D. Mordehai, E. Clouet, M. Fivel, and M. Verdier, Philos. Mag. **88**, 899 (2008).
[56] R. Lagneborg, Scr. Metall. **7**, 605 (1973).
[57] G. L. Reynolds, W. B. Beeré, and B. Burton, Metal Sci. **11**, 213 (1977).
[58] R. J. Amodeo and N. M. Ghoniem, Phys. Rev. B **41**, 6958 (1990).
[59] A. S. Argon, F. Prinz, and W. C. Moffatt, in *Creep and Fracture of Engineering Materials and Structures*, edited by B. Wilshire and D. R. J. Owen (Pineridge, Swansea, 1981), p. 1.
[60] F. Roters, D. Raabe, and G. Gottstein, Comput. Mater. Sci. **7**, 56 (1996).